Original article

Vertical Mixing in the Lower Part of Main Pycnocline in the Black Sea

A. N. Morozov

Marine Hydrophysical Institute of RAS, Sevastopol, Russian Federation anmorozov@mhi-ras.ru

Abstract

Purpose. This study aims to evaluate the vertical turbulent diffusion coefficient in the lower part of the main pycnocline in the areas of continental slope and deep waters of the Black Sea.

Methods and Results. Data were collected during the 87th cruise of R/V Professor Vodyanitsky in the central sector of the northern Black Sea from June 30 to July 18, 2016. Profiles of temperature, salinity, and current velocity were obtained using CTD/LADCP probes. A method applying the G03 parameterization to a layer ~ 200 m thick, spanning isopycnals with conditional densities between 15.5 and 16.8 kg/m³, is proposed. To suppress measurement noise, isopycnal averaging across the station ensemble and approximation of the resulting parameter profiles using power functions were employed. Differences in the transfer functions for CTD and LADCP data processing were accounted for when integrating the canonical spectrum of internal waves. Data from 20 deep-sea stations enabled the derivation of buoyancy frequency profile averaged over the isopycnals, revealing layers of its power and exponential dependences on depth. The methodological challenges of applying the G03 parameterization to the lower part of the Black Sea's main pycnocline are discussed in detail, including graphical data presentation. The profiles of the vertical turbulent diffusion coefficient K_{G03} indicate a nearly constant value of $\sim 2.10^{-6}$ m²/s in the continental slope region, while in the deep waters of the sea, it increases linearly with depth from $1 \cdot 10^{-6}$ m²/s to $2 \cdot 10^{-6}$ m²/s. The maximum calculated heat flux reaches 12 mW/m², confirming its negligible impact on the heating of the cold intermediate layer. The salt flux at the upper boundary of the layer is 6·10⁻⁵ g/(m²·s) in the continental slope region and $\sim 3.10^{-5}$ g/(m²·s) in the deep waters. At the lower boundary of the layer, salt fluxes are nearly identical in both regions, approximately $\sim 5 \cdot 10^{-6}$ g/(m²·s). The shear-to-strain ratio exhibits a pronounced increase with depth, highlighting significant differences in the characteristics of smallscale processes at the boundaries of the lower part of the main pycnocline.

Conclusions. The vertical turbulent diffusion coefficient estimated using the G03 parameterization agrees well with the values obtained from the microstructural sounding in other marine regions. However, the comparability of these estimates remains unresolved and requires synchronous measurements using microstructural and CTD/LADCP probes.

Keywords: Black Sea, main pycnocline, vertical turbulent mixing, Rim Current, current velocity shear, strain

Acknowledgements: The study was conducted within the framework of the state assignment theme of FSBSI FRC MHI FNNN-2024-0012 "Operational Oceanology".

For citation: Morozov, A.N., 2025. Vertical Mixing in the Lower Part of Main Pycnocline in the Black Sea. *Physical Oceanography*, 32(5), pp. 601-612.

© 2025, A. N. Morozov

© 2025, Physical Oceanography

Introduction

Vertical turbulent mixing significantly influences the intensity of biogeochemical processes in the marine environment [1] and plays a critical role in the formation of water masses, maintenance of stratification and modulation of

ISSN 1573-160X PHYSICAL OCEANOGRAPHY VOL. 32 ISS. 5 (2025)





ocean circulation [2]. These factors explain the sustained interest of oceanographers in studying its characteristics under natural conditions over many decades [3].

Vertical mixing in a stratified marine environment is primarily driven by the breaking of internal waves and shear instability [4]. The majority of turbulent energy is concentrated at scales of less than one meter [4, 5], necessitating measurements with centimeter-scale resolution [6]. Currently, estimates of vertical turbulent mixing parameters derived from microstructural probe data are considered the most reliable [1]. However, the use of microstructural probes is limited by the high cost of equipment and the time-intensive nature of measurements [7]. In the deep part of the Black Sea, such measurements have been concluded only three times [1, 8, 9]. In the oxycline, the vertical turbulent diffusion coefficient ranged from $(1-4)\cdot 10^{-6}$ m²/s [8], while in the main pycnocline, data from a single station indicated values of $(4-6)\cdot 10^{-6}$ m²/s [1]. Overall, measurements using microstructural probes suggest a relatively low intensity of vertical mixing in the main pycnocline of the Black Sea.

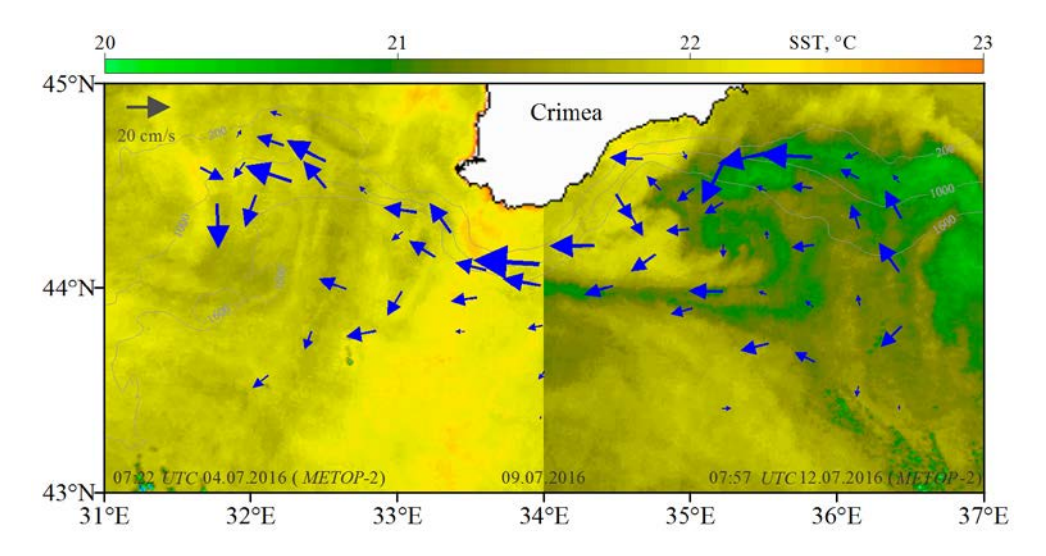
An alternative estimate of the vertical turbulent diffusion coefficient can be derived from synchronous measurements of density and current velocity profiles with a depth resolution of ~ 10 m. For example, in the Black Sea, data from an autonomous Aqualog probe deployed at the shelf edge near Gelendzhik [10] were used to investigate the temporal variability of vertical mixing through a parameterization based on Richardson number values [11, 12]. Another source of such data are areal hydrological surveys conducted during expeditions of Marine Hydrophysical Institute since 2004 [13]. These data are expected to provide new preliminary insights into the spatial structure of vertical mixing parameters.

This study aims to investigate the vertical distribution of turbulent mixing parameters in the main pycnocline across the continental slope and deep part of the Black Sea. To estimate the vertical turbulent diffusion coefficient, the G03 parameterization [14] was applied. This parameterization was selected due to the strong agreement between the calculated vertical turbulent mixing parameters and values derived from microstructural probe measurements [6, 7, 15–17]. The parameterization was introduced in the theoretical work [18], further developed in [19] and presented in its final form in [14]. In modern scientific literature, this parameterization is sometimes referred to as GHP (Gregg – Henyey – Polzin).

Instruments and data

This study uses data on salinity, temperature and current velocity collected during the 87th cruise of the R/V *Professor Vodyanitsky*, conducted in the northern part of the Black Sea (31–36.5°E, 43–45°N) from June 30 to July 18, 2016. Temperature and salinity profiles were measured using an SBE 911plus CTD probe with a depth resolution of 1 m. Horizontal current velocity components were measured with a lowered acoustic Doppler current profiler (LADCP), specifically the WHM300 by RDI. The following operating parameters of the profiler were set as follows: bin size of 4 m, application of the broadband method, time discretization of 1 s and a lowering/raising velocity of ~ 0.5 m/s. Data processing was performed taking in accordance with the recommendations in [13]. A total of

106 stations were sampled, with LADCP/CTD measurements conducted to a depth of at least 350 m at 65 stations (Fig. 1); at 20 stations, CTD measurements extended to a depth of 1900 m [20].



F i g. 1. Station locations against the background of the sea surface temperature (SST) distribution during the 87th cruise of R/V *Professor Vodyanitsky*. Blue arrows show current velocity at a depth of 12 m, with arrow tips corresponding to station positions (65 stations total)

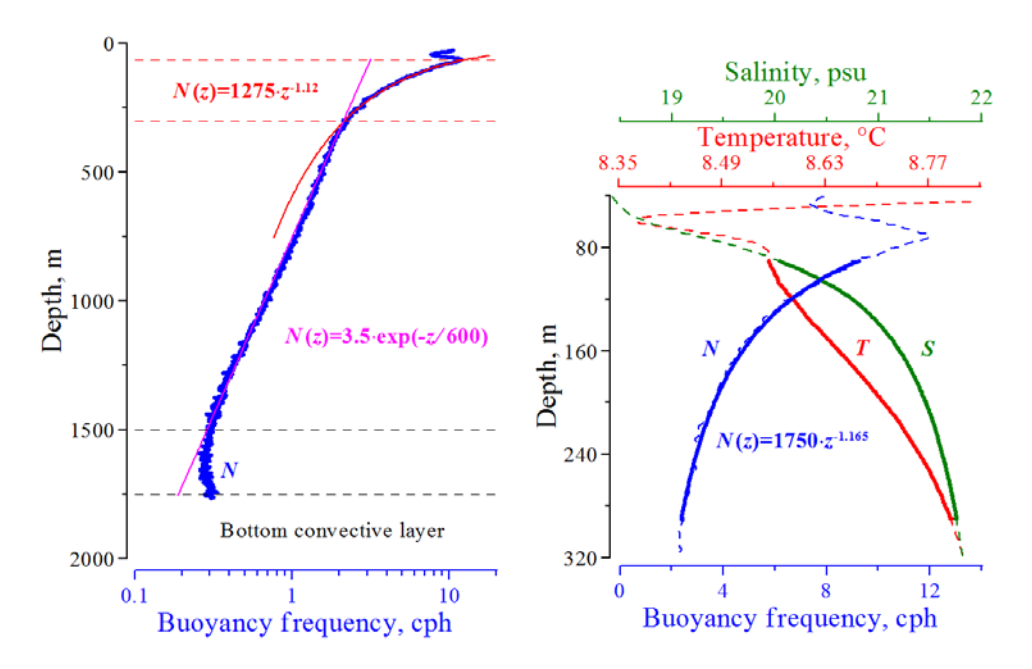
<u>Water dynamics</u>. The current velocity distribution at a depth of 12 m (Fig. 1) qualitatively confirms the cyclonic nature of the large-scale circulation in the Black Sea within the measurement area. The highest velocities were observed near the southern coast of the Crimean Peninsula. No distinct eddy formations were identified. During the cruise, measurements were conducted with nearly equal coverage of both the continental slope and the deep part of the sea.

<u>Hydrology.</u> It is well established that in the main pycnocline of the Black Sea, isopycnal surfaces exhibit a domed shape due to the cyclonic nature of the large-scale circulation [21]. Their depth increases from the center of the sea towards the periphery. In the measurement area, the depth difference of an isopycnal surface can reach 70 m or more [22]. In this study, isopycnal averaging was applied to mitigate the influence of the domed shape of isopycnal surfaces on the accuracy of averaged hydrological parameter profiles.

The isopycnal averaging algorithm is as follows. The conditional density profile (σ_t) from the station with the deepest CTD measurement was used as the reference set of values. For each value, an array of initial data was constructed for the entire station ensemble using linear interpolation, and the mean values of the parameters, including depth, were calculated. This approach ensured a relatively uniform depth resolution for the isopycnally averaged dependencies.

To calculate the vertical turbulent diffusion coefficient (K) within a specific layer, isopycnal averaging of the buoyancy frequency ($N^2 = g \cdot \rho_z/\rho$, where g is

the acceleration due to gravity, ρ is the reference density, ρ_z is its vertical derivative) was performed using an ensemble of 20 deep-sea CTD profiles (Fig. 2, left). Note that such deep-sea measurements in the Black Sea are extremely rare [23], which partially motivated the presentation of the averaged profile across the entire water column. The layer exhibiting a power-law dependence of N on depth (red line) is highlighted by red dashed lines and is the focus of this study. Other researchers have observed a power-law dependence extending to a depth of 750 m [24], which may result from averaging over depth horizons. From 350 to 1500 m, N demonstrates an exponential dependence on depth (purple line). The parameters of this dependence differ slightly from those used in the canonical internal wave spectrum GM76 [25, 26]. The layer below 1500 m is examined in detail in [20]. To provide a clearer visualization of the layer under consideration (highlighted by solid colored lines), Fig. 2, right presents profiles of temperature (T), salinity (S) and buoyancy frequency (N), isopycnally averaged over an ensemble of 65 stations. Although the power-law dependence of the buoyancy frequency on depth is observed within the conditional density range of 15-16.8 kg/m³, the isopycnal surface at $\sigma_t = 15.5$ kg/m³ was selected as the upper boundary of the layer under consideration. This choice is attributed to the emergence of a pronounced dependence on horizontal coordinates in the distribution of N on isopycnal surfaces near $\sigma_t = 15 \text{ kg/m}^3$ [27]. For these calculations, a different mathematical approach is used compared to the one applied in this study.



F i g. 2. Buoyancy frequency profile averaged over the isopycnal surfaces of the 20-station ensemble (left) and temperature, salinity and buoyancy frequency profiles averaged over the isopycnal surfaces of the 65-station ensemble (right)

Further in the work, the stations were divided into two subgroups: one located in the continental slope area (29 stations) with depths less than 1600 m, and the other in the deep part of the sea (36 stations) with depths greater than 1600 m.

Equations and initial data

The applied formulas for calculating the vertical turbulent diffusion coefficient K_{603} are taken from [28]:

$$\begin{split} K_{G03} &= K_0 \cdot \left(\left\langle Sh_{LADCP}^2 \right\rangle \middle/ Sh_{GM \, 76^*}^2 \right)^2 \cdot h_1 \left(R_{\odot} \right) \cdot j \left(f \middle/ \left\langle N \right\rangle \right) = \\ &= K_{G89} \cdot h_1 \left(R_{\odot} \right) \cdot j \left(f \middle/ \left\langle N \right\rangle \right), \\ h_1 (R_{\odot}) &= \frac{3 (R_{\odot} + 1)}{2 \sqrt{2} R_{\odot} \sqrt{R_{\odot} - 1}}, \\ j \left(f \middle/ \left\langle N \right\rangle \right) &= \frac{f \cdot \operatorname{arch} \left(\left\langle N \right\rangle \middle/ f \right)}{f_{30} \cdot \operatorname{arch} \left(N_0 \middle/ f_{30} \right)}, \end{split}$$

where $K = 5 \cdot 10^6$ m²/s; $\langle Sh_{LADCP}^2 \rangle$ is the mean value of the measured shear square; $(Sh^2 = U_z^2 + V_z^2)$, (U_z, V_z) are the depth (z) derivatives of the east and north components of the current velocity; K_{G89} is the coefficient value for the G89 parameterization; f_{30} is the inertial frequency at 30°N; $N_0 = 5.24 \cdot 10^{-3}$ rad/s; f is the local inertial frequency at 44°N; angle brackets denote averaging over the station ensemble. Sh_{GM76*}^2 was calculated for GM76 taking into account the depth resolution of LADCP measurements:

$$Sh_{GM76^*}^2 = \int_{0}^{100} F_{Sh_GM76}(k) \cdot H_{M_ADCP}(k) \cdot H_{Dif_LADCP}(k) \cdot H_{DP_LADCP}(k) \cdot k,$$

where $F_{Sh_GM76}(k)$ is the spectrum of current velocity shears GM76 [30] in the space of vertical wavenumbers (k); $H_{M_ADCP}(k) = (\sin(\pi 4k)/(\pi 4k))^4$ is the transfer function of spatial averaging inherent to ADCP; $H_{Dif_LADCP}(k) = (\sin(\pi 4k)/(\pi 4k))^2$ is the transfer function of differentiation at a depth increment of 4 m; $H_{DP_LADCP}(k) = (\sin(\pi 4k)/(\pi 4k))^4$ is the transfer function of the window-type filter used in data processing. The shear-to-strain ratio $R_{\infty} = \frac{Sh^2}{N^2 \cdot \zeta_z^2}$ [19] (ζ_z is strain, the vertical derivative of the isopycnal displacement

from the equilibrium position) is interpreted as the ratio of kinetic and potential energy of internal waves and for GM76 it equals 3 [30]. The calculation of R_{ω} was carried out taking into account the difference in transfer functions when processing density and current velocity data from the following relation:

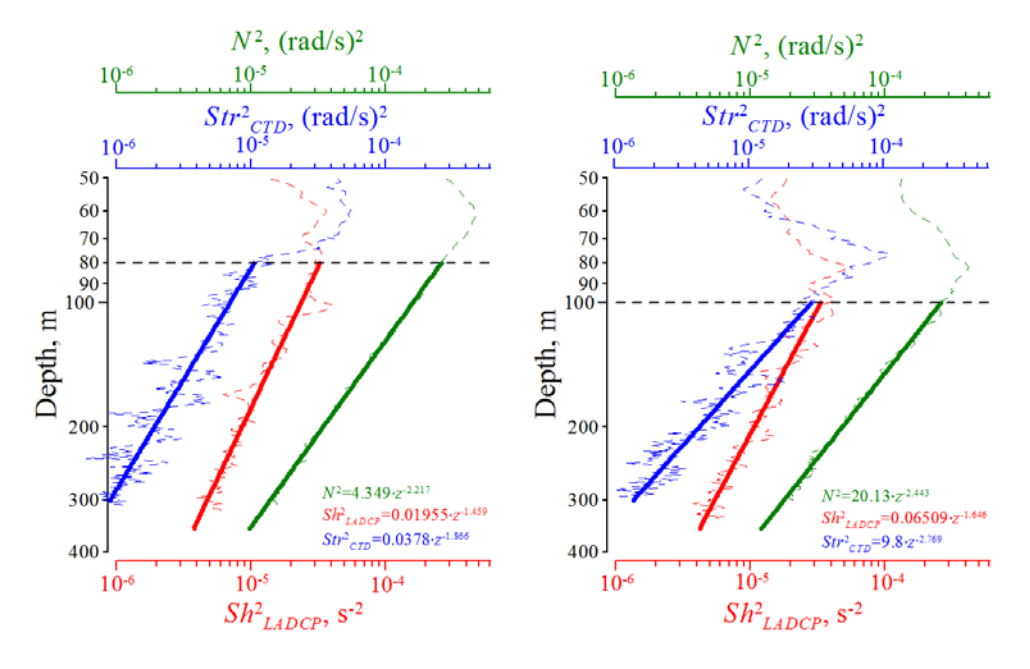
$$R_{\omega} \approx \frac{Sh_{GM76}^2}{\left\langle N^2 \right\rangle \cdot \zeta_{z_GM76}^2} \cdot \frac{\left\langle Sh_{LADCP}^2 \right\rangle / Sh_{GM76^*}^2}{\left\langle \zeta_{z_CTD}^2 \right\rangle / \zeta_{z_GM76^*}^2} = 3 \cdot \frac{\left\langle Sh_{LADCP}^2 \right\rangle}{\left\langle N^2 \right\rangle \cdot \left\langle \zeta_{z_CTD}^2 \right\rangle} \cdot \frac{\left\langle N^2 \right\rangle \cdot \zeta_{z_GM76^*}^2}{Sh_{GM76^*}^2},$$

where $\zeta_{z_{-CTD}}^2 = \left\langle \left(N^2 - \left\langle N^2 \right\rangle \right)^2 \right\rangle / \left\langle N^2 \right\rangle^2$ is the measured value of the square of strain

[19];
$$\zeta_{z_{-}GM76^{*}}^{2} = \int_{0}^{100} F_{\zeta_{z_{-}}GM76}(k) \cdot H_{Dif_{-}CTD}(k) \cdot H_{DP_{-}CTD}(k) \cdot dk$$
, $F_{\zeta_{z_{-}}GM76}(k)$ is

the strain spectrum GM76 [30], $H_{Dif_CTD}(k) = (\sin(\pi 4k)/(\pi 4k))^2$ is the transfer function of differentiation at a depth increment of 4 m, $H_{DP_CTD}(k) = (\sin(\pi k)/(\pi k))^4$ is the transfer function of CTD data processing. After appropriate integration, we obtain the relation that was applied in the calculations, $R_{\omega} \approx 2.1 \cdot \frac{\left\langle Sh_{LADCP}^2 \right\rangle}{\left\langle N^2 \right\rangle \cdot \left\langle \zeta_{z_CTD}^2 \right\rangle} = 2.1 \cdot \frac{\left\langle Sh_{LADCP}^2 \right\rangle}{\left\langle Str_{CTD}^2 \right\rangle}$. The value Str_{CTD}^2 is

introduced for the convenience of graphical representation.



F i g. 3. Profiles of N^2 , Str_{CTD}^2 and Sh_{LADCP}^2 (dashed lines) averaged over the isopycnal surfaces and their approximations by power functions (solid lines) for the deep-sea part (*left*) and the continental slope (*right*)

In the layer under consideration, the dependencies $N^2(z)$, $Sh_{LADCP}^2(z)$, $Str_{CTD}^2(z)$ are well represented by power functions (Fig. 3). This result is unexpected and may reflect a pattern characteristic of this layer. Notably, the most significant difference

between the center of the sea and the continental slope is observed in the dependence for $Str_{CTD}^2(z)$.

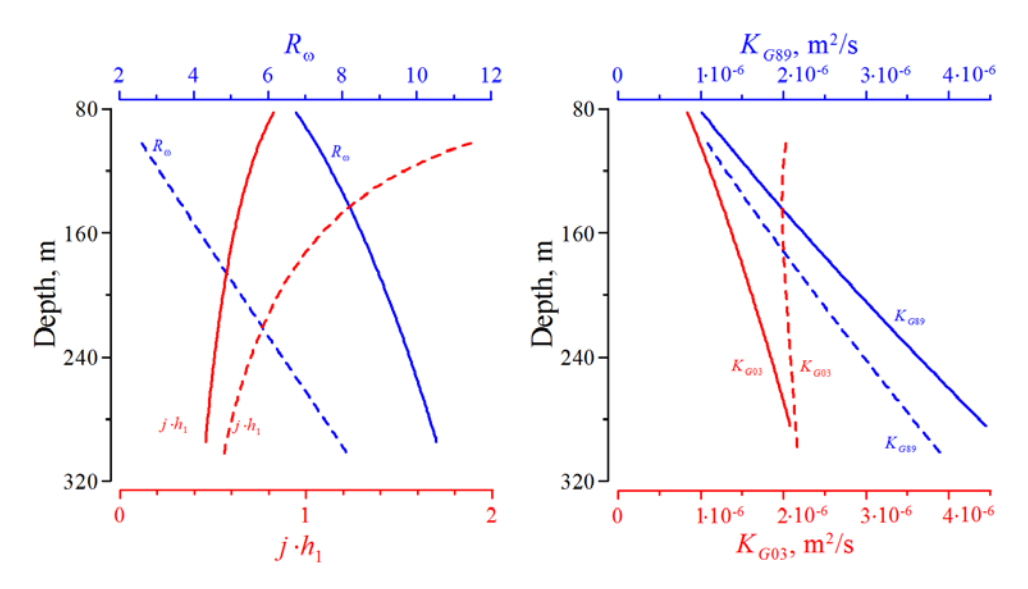
Preliminary data processing involved averaging the parameters over isopycnal surfaces and approximating them with power functions to suppress the random component of measurement noise and errors in estimating the mean values of random processes from a relatively small sample. Subsequently, when estimating K, power-law dependencies were used; for this purpose, $\langle N^2 \rangle$, $\langle N \rangle$, $\langle Sh_{LADCP}^2 \rangle$, $Sh_{GM76^*}^2$, $\langle Str_{CTD}^2 \rangle$, $Str_{GM76^*}^2$ in the formulas were replaced by their approximating functions (Fig. 3).

Results and discussion

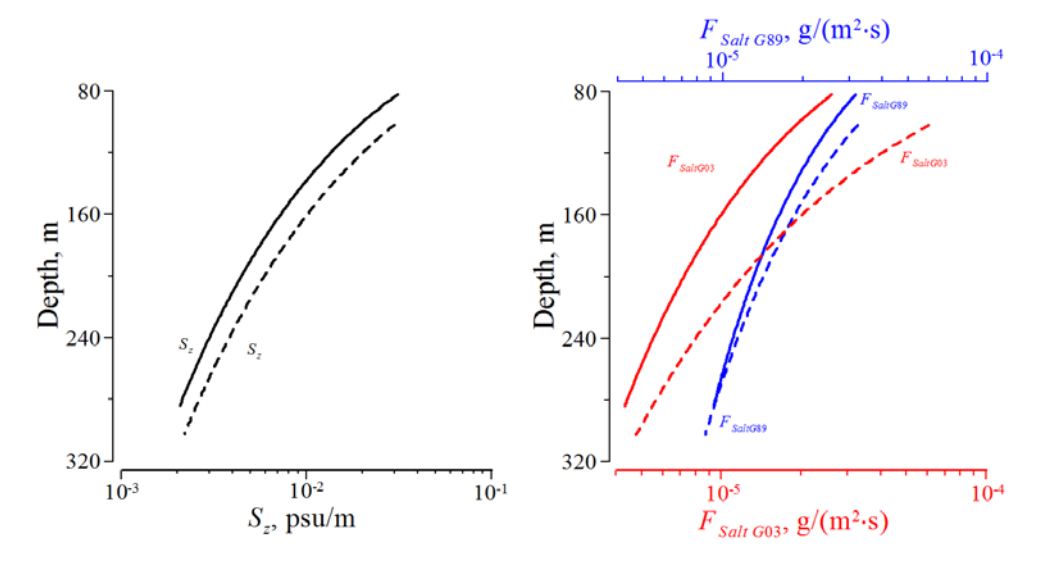
This study examines the behavior of G03 parameterization factors within the specified layer (Fig. 4, *left*). The shear-to-strain ratio, which is critical for estimating K_{G03} [31], increases with depth in both the deep part of the sea and the continental slope region. However, in the deep part, the values of R_{\odot} are higher, potentially due to the influence of internal waves with frequencies close to inertial [32–34], where kinetic energy significantly exceeds potential energy [35]. As a result, the factor $j \cdot h_1$ in the deep part decreases by a factor of two, whereas in the continental slope region, it decreases by nearly a factor of five. This results in K_{G03} values in the central part of the sea increasing with depth from $1 \cdot 10^{-6}$ to $2 \cdot 10^{-6}$ m²/s, while in the continental slope region, it remains nearly constant, at $\sim 2 \cdot 10^{-6}$ m²/s. The earlier G89 parameterization, which is proportional to the fourth power of the ratio of measured shear to its value for GM76, yields similar dependencies of K_{G89} for the deep part of the sea and the continental slope.

Compared to estimates derived from microstructural probe measurements [1,8], the G03 and G89 parameterizations demonstrate strong comparability. In terms of the depth dependence of K, the G03 parameterization shows greater consistency. However, the comparability of K estimates obtained from microstructural probe data and standard CTD/LADCP measurements in the Black Sea remains unresolved due to the absence of synchronous measurement results.

The determination of the vertical turbulent diffusion coefficient is partly driven by the need to estimate vertical fluxes of various substances in the marine environment to better understand the mechanisms of their stratification. In this study, based on the calculated K_G values, an estimate of the salt flux was performed (Fig. 5, right), calculated using the relation $F_{SaltG} = \rho \cdot K_G \cdot S_z$, where S_z is the vertical derivative of salinity (Fig. 5, left). The salt flux $F_{SaltG03}$ at the upper boundary of the layer in the deep part of the sea is nearly twice as high as in the continental slope region. At the lower boundary, its values are approximately the same for both regions.

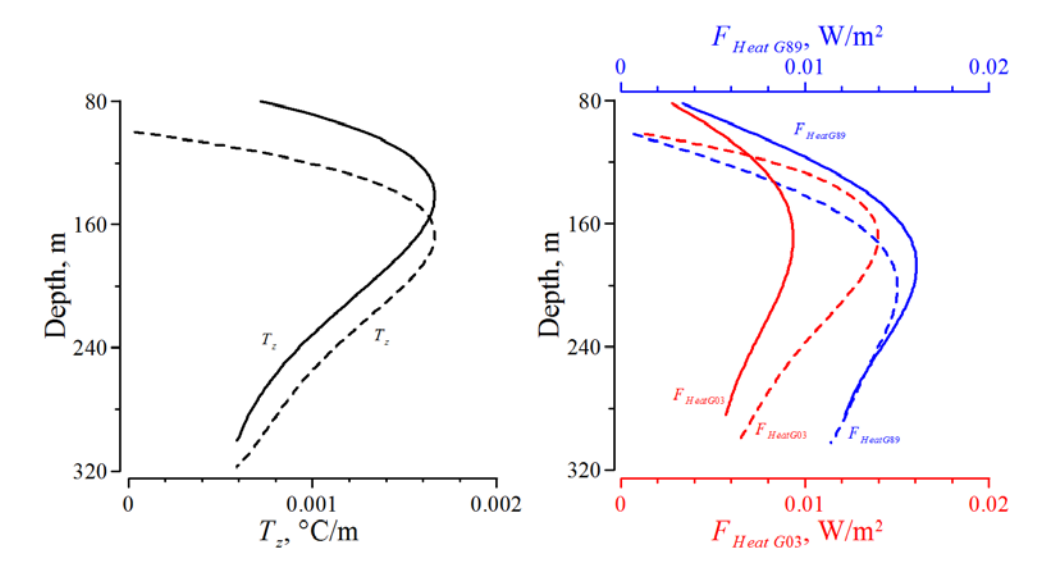


F i g. 4. Profiles of R_{∞} and j h_1 (*left*) and resulting profiles of the vertical turbulent diffusion coefficient for G03 and G89 parameterizations (*right*). Solid lines show deep part of the sea, dashed lines represent continental slope



F i g. 5. Profiles of the vertical derivative of salinity (*left*) and salt fluxes (*right*) for the deep-sea part (solid lines) and the continental slope (dashed lines)

The heat flux was calculated from the relation $F_{HeatG} = \rho \cdot C_W \cdot K_G \cdot T_z$, where $C_W = 4200$ J/(°C·kg) is the heat capacity of water, T_z is the vertical derivative of temperature (Fig. 6, left). The G03 and G89 parameterizations yield relatively low heat flux values for both regions, with a maximum of ~ 16 mW/m² (Fig. 6, right). Essentially, this suggests that the heat flux from the sea depths has a negligible effect on the warming of the cold intermediate layer.



F i g. 6. Profiles of the vertical derivative of water temperature (*left*) and heat fluxes (*right*) for the deep-sea part (solid lines) and the continental slope (dashed lines)

Conclusion

This paper presents a method for applying the G03 parameterization to estimate the vertical turbulent diffusion coefficient in a layer ~ 200 m thick using standard CTD/LADCP measurement data. To suppress the random component of measurement noise, isopycnal averaging over the station ensemble and approximation of the resulting profiles by power-law functions were used. The differences in the transfer functions of CTD and LADCP data processing were considered when integrating the canonical internal wave spectrum GM76.

The resulting profiles of the vertical turbulent diffusion coefficient K_{G03} indicate a nearly constant value of $\sim 2\cdot 10^{-6}$ m²/s in the continental slope region and a linear increase with depth from $1\cdot 10^{-6}$ to $2\cdot 10^{-6}$ m²/s in the deep part of the sea. Despite the relatively low values of the coefficient, they align well with estimates obtained from microstructural probe measurements.

The calculated heat fluxes exhibit low values, with a maximum of 12 mW/m^2 , confirming their negligible influence on the warming of the cold intermediate layer. The salt flux at the upper boundary of the layer in the continental slope region is $6 \cdot 10^{-5} \text{ g/(m}^2 \cdot \text{s})$, while in the deep part of the sea, it is $\sim 3 \cdot 10^{-5} \text{ g/(m}^2 \cdot \text{s})$. At the lower boundary of the layer, the salt fluxes are nearly identical for both regions, $\sim (4-5) \cdot 10^{-6} \text{ g/(m}^2 \cdot \text{s})$.

In the lower part of the Black Sea's main pycnocline, a sharp increase in the shear-to-strain ratio with depth is observed, potentially resulting from the interaction of internal waves with small-scale inhomogeneities in density stratification.

REFERENCES

- Zatsepin, A.G., Golenko, N.N., Korzh, A.O., Kremenetskii, V.V., Paka, V.T., Poyarkov, S.G. and Stunzhas, P.A., 2007. Influence of the Dynamics of Currents on the Hydrophysical Structure of the Waters and the Vertical Exchange in the Active Layer of the Black Sea. *Oceanology*, 47(3), pp. 301-312. https://doi.org/10.1134/S0001437007030022
- Munk, W.H., 1966. Abyssal Recipes. Deep Sea Research and Oceanographic Abstracts, 13(4), pp. 707-730. https://doi.org/10.1016/0011-7471(66)90602-4
- 3. Munk, W.H. and Anderson, E.R., 1948. Notes on the Theory of the Thermocline. *Journal of Marine Research*, 7(3), pp. 276-295.
- Polzin, K.L., Naveira Garabato, A.C., Huussen, T.N., Sloyan, B.M. and Waterman, S., 2014. Finescale Parameterizations of Turbulent Dissipation. *Journal of Geophysical Research: Oceans*, 119(2), pp. 1383-1419. https://doi.org/10.1002/2013JC008979
- Le Boyer, A., Couto, N., Alford, M.H., Drake, H.F., Bluteau, C.E., Hughes, K.G., Naveira Garabato, A.C., Moulin, A.J., Peacock, T. [et al.], 2023. Turbulent Diapycnal Fluxes as a Pilot Essential Ocean Variable. Frontier in Marine Science, 10, 1241023. https://doi.org/10.3389/fmars.2023.1241023
- Sasaki, Y., Yasuda, I., Katsumata, K., Kouketsu, S. and Uchida, H., 2024. Turbulence across the Antarctic Circumpolar Current in the Indian Southern Ocean: Micro-Temperature Measurements and Finescale Parameterizations. *Journal of Geophysical Research: Oceans*, 129(2), e2023JC019847. https://doi.org/10.1029/2023JC019847
- Takahashi, A. and Hibiya, T., 2018. Assessment of Finescale Parameterizations of Deep Ocean Mixing in the Presence of Geostrophic Current Shear: Results of Microstructure Measurements in the Antarctic Circumpolar Current Region. *Journal of Geophysical Research: Oceans*, 124(1), pp. 135-153. https://doi.org/10.1029/2018JC014030
- Gregg, M.C. and Yakushev, E., 2005. Surface Ventilation of the Black Sea's Cold Intermediate Layer in the Middle of the Western Gyre. *Geophysical Research Letters*, 32(3), 2004GL021580. https://doi.org/10.1029/2004GL021580
- 9. Samodurov, A.S., Chukharev, A.M., Kazakov, D.A., Pavlov, M.I. and Korzhuev, V.A., 2023. Vertical Turbulent Exchange in the Black Sea: Experimental Studies and Modeling. *Physical Oceanography*, 30(6), pp. 689-713.
- Zatsepin, A.G., Ostrovskii, A.G., Kremenetskiy, V.V., Nizov, S.S., Piotukh, V.B., Soloviev, V.A., Shvoev, D.A., Tsibul'sky, A.I., Kuklev, S.B. [et al.], 2014. Subsatellite Polygon for Studying Hydrophysical Processes in the Black Sea Shelf-Slope Zone. *Izvestiya, Atmospheric and Oceanic Physics*, 50(1), pp. 13-25. https://doi.org/10.1134/S0001433813060157
- Podymov, O.I., Zatsepin, A.G. and Ostrovsky, A.G., 2017. Vertical Turbulent Exchange in the Black Sea Pycnocline and Its Relation to Water Dynamics. *Oceanology*, 57(4), pp. 492-504. https://doi.org/10.1134/S0001437017040142
- Podymov, O.I., Zatsepin, A.G. and Ostrovskii, A.G., 2023. Fine Structure of Vertical Density Distribution in the Black Sea and Its Relationship with Vertical Turbulent Exchange. *Journal of Marine Science and Engineering*, 11(1), 170. https://doi.org/10.3390/jmse11010170
- 13. Morozov, A.N. and Lemeshko, E.M., 2006. Methodical Aspects of the Application of Acoustic Doppler Current Profilers in the Black Sea. *Physical Oceanography*, 16(4), pp. 216-233. https://doi.org/10.1007/s11110-006-0027-8
- Gregg, M.C., Sanford, T.B. and Winkel, D.P., 2003. Reduced Mixing from the Breaking of Internal Waves in Equatorial Waters. *Nature*, 422, pp. 513-515. https://doi.org/10.1038/nature01507
- Ferron, B., Kokoszka, F., Mercier, H. and Lherminier, P., 2014. Dissipation Rate Estimates from Microstructure and Finescale Internal Wave Observations along the A25 Greenland– Portugal OVIDE Line. *Journal of Atmospheric and Oceanic Technology*, 31(11), pp. 2530-2543. https://doi.org/10.1175/JTECH-D-14-00036.1

- Fine, E.C., Alford, M.H., MacKinnon, J.A. and Mickett, J.B., 2021. Microstructure Mixing Observations and Finescale Parameterizations in the Beaufort Sea. *Journal of Physical Oceanography*, 51(1), pp. 19-35. https://doi.org/10.1175/JPO-D-19-0233.1
- 17. Baumann, T.M., Fer, I., Schulz, K. and Mohrholz, V., 2023. Validating Finescale Parameterizations for the Eastern Arctic Ocean Internal Wave Field. *Journal of Geophysical Research: Oceans*, 128(11), e2022JC018668. https://doi.org/10.1029/2022JC018668
- Henyey, F.S., Wright, J. and Flatté, S.M., 1986. Energy and Action Flow through the Internal Wave Field: An Eikonal Approach. *Journal of Geophysical Research: Oceans*, 91(C7), pp. 8487-8495. https://doi.org/10.1029/JC091iC07p08487
- 19. Polzin, K.L., Toole, J.M. and Smith, R.W., 1995. Finescale Parameterizations of Turbulent Dissipation. *Journal of Physical Oceanography*, 25(3), pp. 306-328. https://doi.org/10.1175/1520-0485(1995)025<0306:FPOTD>2.0.CO;2
- Morozov, A.N. and Mankovskaya, E.V., 2022. Characteristics of the Bottom Convective Layer of the Black Sea Based on in-situ Data (July, 2016). *Physical Oceanography*, 29(5), pp. 524-535. https://doi.org/10.22449/1573-160X-2022-5-524-535
- 21. Ivanov, V.A. and Belokopytov, V.N., 2013. *Oceanography of the Black Sea*. Sevastopol: ECOSY-Gidrofizika, 210 p.
- Morozov, A.N. and Mankovskaya, E.V., 2021. Spatial Characteristics of the Black Sea Cold Intermediate Layer in Summer, 2017. *Physical Oceanography*, 28(4), pp. 404-413. https://doi.org/10.22449/1573-160X-2021-4-404-413
- 23. Stanev, E.V., Chtirkova, B. and Peneva, E., 2021. Geothermal Convection and Double Diffusion Based on Profiling Floats in the Black Sea. *Geophysical Research Letters*, 48(2), e2020GL091788. https://doi.org/10.1029/2020GL091788
- Samodurov, A.S., 2016. Complimentarity of Different Approaches for Assessing Vertical Turbulent Exchange Intensity in Natural Stratified Basins. *Physical Oceanography*, (6), pp. 32-42. https://doi.org/10.22449/1573-160X-2016-6-32-42
- Garrett, C. and Munk, W., 1975. Space-Time Scales of Internal Waves: A Progress Report. *Journal of Geophysical Research*, 80(3), pp. 291-297. https://doi.org/10.1029/JC080i003p00291
- Cairns, J.L. and Williams, G.O., 1976. Internal Wave Observations from a Midwater Float, 2. *Journal of Geophysical Research*, 81(12), pp. 1943-1950. https://doi.org/10.1029/JC081i012p01943
- 27. Morozov, A.N., 2025. Vertical Mixing in the Main Pycnocline of the Black Sea in Summer. *Physical Oceanography*, 32(3), pp. 271-282.
- 28. Kunze, E., Firing, E., Hummon, J.M., Chereskin, T.K. and Thurnherr, A.M., 2006. Global Abyssal Mixing Inferred from Lowered ADCP Shear and CTD Strain Profiles. *Journal of Physical Oceanography*, 36(8), pp. 1553-1576. https://doi.org/10.1175/JPO2926.1
- 29. Gregg, M.C., 1989. Scaling Turbulent Dissipation in the Thermocline. *Journal of Geophysical Research: Oceans*, 94(C7), pp. 9686-9698. https://doi.org/10.1029/JC094iC07p09686
- 30. Fer, I., 2006. Scaling Turbulent Dissipation in an Arctic Fjord. *Deep Sea Research Part II: Topical Studies in Oceanography*, 53(1-2), pp. 77-95. https://doi.org/10.1016/j.dsr2.2006.01.003
- 31. Chinn, B.S., Girton, J.B. and Alford, M.H., 2016. *The* Impact of Observed Variations in the Shear-to-Strain Ratio of Internal Waves on Inferred Turbulent Diffusivities. *Journal of Physical Oceanography*, 46(11), pp. 3299-3320. https://doi.org/10.1175/JPO-D-15-0161.1
- 32. Zhurbas, V.M., Zatsepin, A.G., Grigor'eva, Yu.V., Poyarkov, S.G., Eremeev, V.N., Kremenetsky, V.V., Motyzhev, S.V., Stanichny, S.V., Soloviev, D.M. [et al.], 2004. Water Circulation and Characteristics of Currents of Different Scales in the Upper Layer of the Black Sea from Drifter Data. *Oceanology*, 44(1), pp. 30-43.
- 33. Khimchenko, E., Ostrovskii, A., Klyuvitkin, A. and Piterbarg, L., 2022. Seasonal Variability of Near-Inertial Internal Waves in the Deep Central Part of the Black Sea. *Journal of Marine Science and Engineering*, 10(5), 557. https://doi.org/10.3390/jmse10050557

- 34. Khimchenko, E. and Ostrovskii, A., 2024. Observations of Near-Inertial Internal Waves over the Continental Slope in the Northeastern Black Sea. *Journal of Marine Science and Engineering*, 12(3), 507. https://doi.org/10.3390/jmse12030507
- 35. Morozov, A.N., Mankovskaya, E.V. and Fedorov, S.V., 2021. Inertial Oscillations in the Northern Part of the Black Sea Based on the Field Observations. *Fundamental and Applied Hydrophysics*, 14(1), pp. 43-53. https://doi.org/10.7868/S2073667321010044 (in Russian).

Submitted 07.11.2024; approved after review 18.02.2025; accepted for publication 11.07.2025.

About the author:

Alexey N. Morozov, Senior Research Associate, Marine Hydrophysical Institute of RAS (2 Kapitanskaya Str., Sevastopol, 299011, Russian Federation), CSc. (Tech.), ORCID ID: 0000-0001-9022-3379, Scopus Author ID: 7202104940, ResearcherID: ABB-4365-2020, SPIN-code: 6359-0395, anmorozov@mhi-ras.ru

The author has read and approved the final manuscript. The author declares that he has no conflict of interest.